Sources and Characterization of Clutter in Cardiac B-mode Images

Muyinatu A. Lediju, Brett C. Byram, and Gregg E. Trahey Department of Biomedical Engineering, Duke University, Durham, NC Email: muyinatu.lediju@duke.edu

Abstract—In echocardiography, clutter is one of the most problematic image artifacts, often obscuring ventricular borders and introducing stationary noise in blood flow measurements. Clutter in transthoracic cardiac images is widely understood to originate from reverberations and off-axis echoes. The objective of this work is to investigate the sources of clutter in cardiac images and their relative contributions. Real-time 3D raw echo data was acquired at a volumetric frame rate of 1 kHz and speckle tracking was applied to resulting images to determine the motion characteristics of clutter and adjacent myocardium. When clutter adjacent to the myocardial wall was tracked, the clutter and adjacent myocardium had similar displacements. When clutter farther from the myocardial wall was tracked, displacements were temporally and spatially complex and did not correlate well with any portion of the myocardium. In addition, principal component analysis (PCA) was applied to the raw echo data and resulting eigenvectors were used to isolate various motion patterns in the cardiac data. Results support the hypothesis that echoes from stationary structures, such as the ribcage and chest wall, are contributors to stationary clutter noise, while the myocardium is a dominant source of nonstationary clutter.

I. BACKGROUND

Clutter is a problematic noise artifact in echocardiography. It obscures endocardial borders, corrupts diagnostic information, and inhibits visualization of tumors, vegetations, and other cardiac abnormalities [1, 2]. Myocardium-to-cavity echo ratios as low as 0.7 have been reported, indicating that clutter noise can be stronger than the myocardium itself [3]. In most cases, clutter noise is stronger than blood signals within myocardial cavities. Clutter sources include reverberations and reflections from extracardiac off-axis structures such as the ribcage and lungs, as well as from intracardiac structures such as the chordae tendineae, valves, and myocardial walls [4, 5, 6].

One method known to reduce clutter in cardiac images is harmonic imaging, in which pulses are transmitted at a fundamental frequency and echoes generated by the nonlinear propagation of sound through tissue are received at a higher harmonic frequency. This technique improves border delineation, contrast measurements, and endocardial visualization [7, 8, 9]. In several studies, the application of harmonic imaging lowered the percentage of patients with suboptimal images due to clutter from 45-51% to 11-24% [10, 11]. However, the fact that a subset of patients still showed suboptimal echocardiograms with harmonic imaging indicates that this technique is not sufficiently effective at reducing clutter.

Additional techniques to reduce clutter in cardiac images are targeted at stationary noise [5, 12, 13], thus ignoring clutter due to moving structures.

II. PREVIOUS WORK

Motion analyses were previously utilized to identify clutter sources in abdominal images [14]. The abdominal wall was axially displaced during successive-frame image acquisitions, and speckle tracking was applied to consecutive frames of raw RF echo data. This was implemented in *in vivo* bladder and gall bladder images, structures that are expected to be hypoechoic or anechoic in the absence of clutter, such that echoes seen within them are assumed to be clutter noise.

Results support hypotheses about the applied motion, that the transducer, abdominal wall, and underlying clutter move approximately in unison while distal tissues remain stationary. In other words, the abdominal wall and a clutter region distal to the abdominal wall were shown to be stationary relative to the transducer, while the distal tissues and adjacent distal clutter regions were shown to move toward the transducer. The dominant stationary clutter region (relative to the transducer) is believed to arise from acoustic interactions within the abdominal wall, such as sound reverberation. Farther away, off-axis scattering appeared to be the dominant clutter source.

III. CLUTTER ASSESSMENT IN CARDIAC IMAGES

Previously-implemented motion analyses were translated to cardiac images to assess and characterize clutter sources. While it is not feasible to displace the chest wall, the beating heart and its associated motion may be used to perform similar motion analyses. It is hypothesized that clutter sources in cardiac images due to stationary structures (e.g. chest wall, ribcage) should appear stationary, while clutter due to lateral and elevational structures in the heart should move with those structures. Concordant clutter and structural motion should appear in 2D and/or 3D speckle tracked images.

To test these hypotheses, raw echo data from real-time 3D cardiac images of the left ventricle of one volunteer (short axis view) were acquired at a volume rate of 1 kHz, utilizing a Siemens Medical Systems SC2000 cardiac scanner with a matrix array. Speckle tracking was applied with kernel sizes measuring 2 mm (lateral) x 2° (lateral) x 2° (elevational). Maps of axial displacements at three specific times in the cardiac cycle are shown in Fig. 1. Early in time (Fig. 1 (a)), the left ventricle is contracting, as evidenced in the corresponding

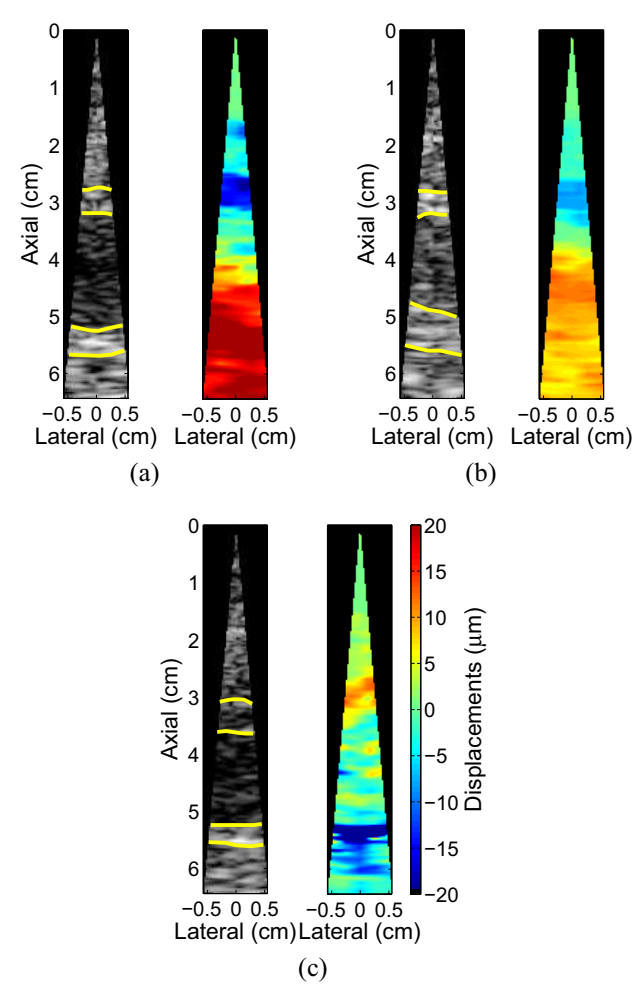


Fig. 1. B-mode images with manually-determined myocardial borders superimposed and corresponding axial displacement maps at (a) 700 ms, (b) 775 ms, and (c) 862 ms.

axial displacement map where proximal and distal myocardia exhibit opposing motion. Later in the cardiac cycle (Fig. 1 (b)), the left ventricle appears to be fully contracted in the B-mode image, and the proximal and distal myocardia still show opposing motion, albeit with reduced magnitudes. Even later (Fig. 1 (c)), the ventricle is shown to undergo relaxation, as evidenced by axial displacement maps showing opposing proximal and distal myocardial motion that is opposite in sign compared to the two earlier cases. Note that regions in the ventricle have similar motion to nearby myocardial tissue.

The displacement data within regions of interest (ROIs) that moved with the myocardium were averaged, cumulatively-summed, and plotted as a function of time. Fig. 2 shows the average axial, lateral, and elevational displacements in proximal and distal myocardium and clutter ROIs for an entire entire cardiac cycle. The proximal myocardium and proximal clutter region have similar axial displacements, as does the distal myocardium and distal clutter region (see Fig. 2 (a)). On the contrary, the ventricular center does not clearly follow the proximal nor distal myocardial wall. Similar conclusions

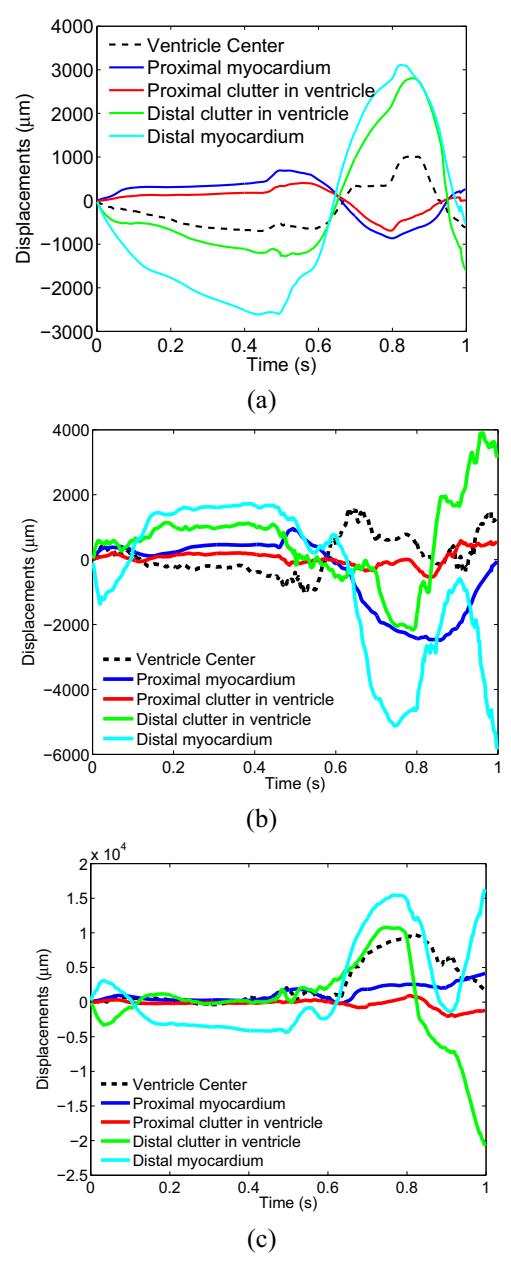


Fig. 2. Cumulatively-summed, average (a) axial, (b) lateral, and (c) elevational displacements throughout the entire cardiac cycle.

can be drawn for lateral (Fig. 2 (b)) and elevational (Fig. 2 (c)) displacements. The displacement in the chest wall region (not shown) was approximately zero for the entire cardiac cycle. In contrast to abdominal images, the displacement estimates show that stationary reverberations are not a dominant source of clutter in the cardiac image.

A 1, -1 finite impulse response (FIR) filter was applied to the cardiac data. The chest wall region was reduced by -35 dB. Axial displacement maps at three specific points in the cardiac cycle are shown in Fig. 3. Similar displacement results are seen when compared to the unfiltered case. Early in the cardiac cycle (Fig. 3 (a)), the ventricle is contracting, as evidenced by the opposing myocardial motion shown in the

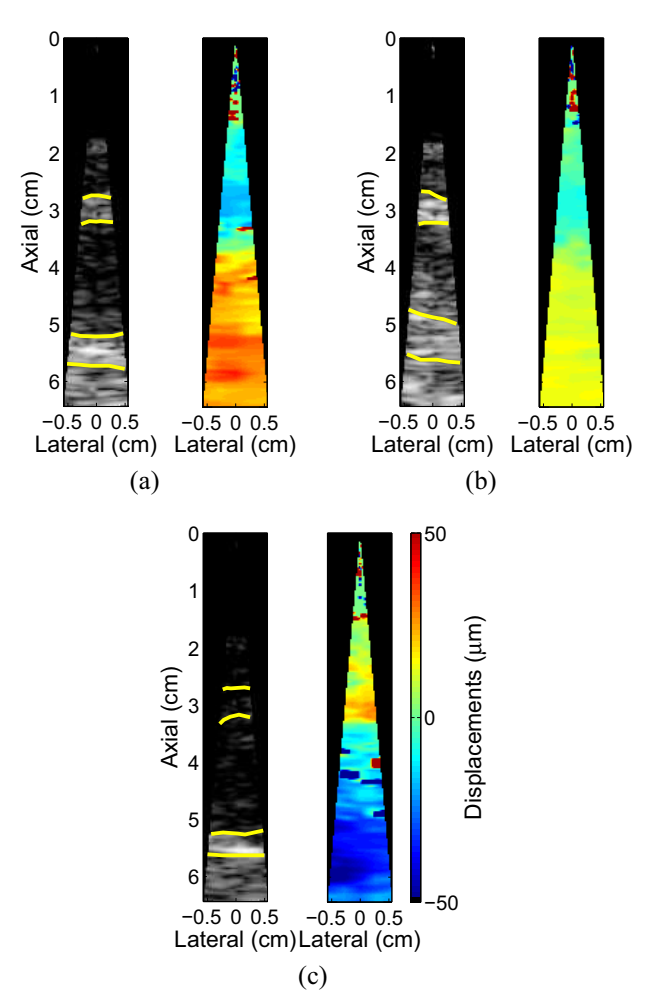


Fig. 3. 1, -1 FIR-filtered B-mode images with manually-determined myocardial borders superimposed and corresponding axial displacement maps at (a) 700 ms, (b) 775 ms, and (c) 866 ms.

axial displacement maps. Later in the cardiac cycle (Fig. 3 (b)), the ventricle appears to be fully contracted, and there is still opposing myocardial motion, albeit with decreased magnitudes. Even later (Fig. 3 (c)), the ventricle appears to undergo relaxation, as the opposing myocardial wall motion has reversed signs. Note that the axial displacement maps show regions in the ventricle that have similar motion to nearby myocardial tissue.

Axial, lateral, and elevational displacements throughout an entire cardiac cycle of 1, -1 FIR-filtered data are shown in Fig. 4. There are similar trends to the pre-filtered case. The axial displacements (Fig. 4 (a)) of the proximal myocardial and clutter regions are moving together, that of the distal regions are moving together, while that of the ventricular center does not move with neither the proximal nor distal myocardial wall. Similarly, in Fig. 4 (b), the proximal regions have similar lateral displacements, the distal regions have similar displacements (although not as similar as in the pre-filtered case), and lateral motion in the ventricular center does not correlate well with either region. Likewise, in Fig. 4

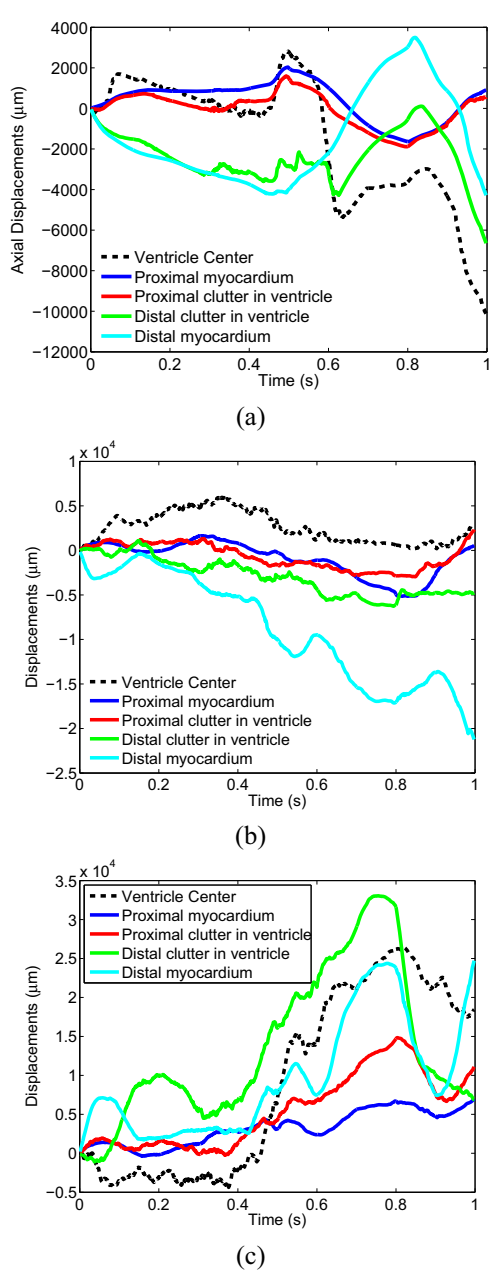


Fig. 4. Cumulatively-summed, average (a) axial, (b) lateral, and (c) elevational displacements in select regions of the FIR-filtered data.

(c), proximal regions have similar elevational displacements, distal regions have similar elevational displacements, and the ventricular center does not have similar motion to either region, especially for large displacement values. In this FIR-filtered case, the axial, lateral, and elevational displacements are larger than respective displacements in the pre-filtered case.

A principal component analysis (PCA) was applied along the axial dimension of RF echoes in an entire data set [15]. As described by Gallippi et al. [16], basis functions associated with a particular principal component (PC) may be used to derive time and depth projections. A time projection describes the motion profile associated with a particular PC, while the corresponding depth projection indicates the relative strength of that PC at each axial position. The 1st PC exhibited a stationary time projection, the 2nd PC exhibited a mostly stationary time projection with subtle motion later in time (similar to the proximal myocardial and clutter displacements shown in Fig. 2 (a) and 4 (a)), and the 3rd and 6th PCs exhibited a time profile similar to that of the distal myocardial and clutter displacements shown in Figs. 2 (a) and 4 (a). Remaining PCs had more complex time projections.

A PCA-based Blind Source Separation [14, 16] was applied to the unfiltered cardiac data, wherein each PC was individually used to reconstruct filtered images (results not shown). An image reconstructed with the 1st PC contained mostly the chest wall and proximal myocardium, confirming that stationary echoes in this cardiac data set are predominantly contained in those regions. An image reconstructed with the 2nd PC contained the chest wall and proximal myocardium, as well as a region extending beyond the proximal myocardial wall. An image reconstructed with the 3rd or 6th PC had its brightest reflectors in the distal myocardium and adjacent clutter region, confirming that these two regions have similar motions. Images reconstructed with remaining principle components excluded the stationary chest wall region and contained a combination of proximal and distal myocardium regions, as well as associated clutter. Results suggest that there are few truly stationary echoes in the ventricular center.

IV. STUDY LIMITATIONS

Results highlight the significance of clutter contributions from myocardial motion. However, there are several limitations associated with this study. First, the myocardial cavity contains structural (e.g. chordae tendineae) and blood echoes as well as clutter noise, and therefore identification of clutter is not as straightforward as in bladder and gall bladder images. Second, clutter caused by slowly-moving extracardiac structures (e.g. lungs) is not easily identifiable and separable from other clutter sources. Furthermore, the limited number of volunteers (n=1) precludes generalization to all patients.

ACKNOWLEDGMENTS

The authors are grateful to Siemens Medical Solutions USA, Inc. for supplying imaging equipment and technical support. Funding was provided by the NIH Supplement to Promote Diversity in Biomedical Research (RO1CA114093-04S1), the NIH National Heart Lung and Blood Institute (R01HL096023), and the Duke Endowment Fellowship.

REFERENCES

- [1] BF Vandenberg, LS Rath, P. Stuhlmuller, HE Melton, and DJ Skorton. Estimation of left ventricular cavity area with an on-line, semiautomated echocardiographic edge detection system. *Circulation*, 86(1):159–166, 1992.
- [2] AK Patel, AV Moorthy, VU Yap, and JH Thomsen. Cardiac metastasis from transitional cell carcinoma: a subtle echocardiographic entity. *J Clin Ultrasound*, 8(1), 1980.

- [3] AC Vançon, ER Fox, CM Chow, J Hill, AE Weyman, MH Picard, and M Scherrer-Crosbie. Pulse inversion harmonic imaging improves endocardial border visualization in two-dimensional images: comparison with harmonic imaging. J Am Soc Echocardiography, 15(4):302–308, 2002.
- [4] EL Yeh. Reverberations in echocardiograms. *J Clin Ultrasound*, 5(2), 1977.
- [5] G Zwirn and S Akselrod. Stationary clutter rejection in echocardiography. *Ultrasound Med Biol*, 32(1):43–52, 2006
- [6] G Cloutier, D Chen, and LG Durand. A new clutter rejection algorithm for Doppler ultrasound. *IEEE Trans Med Imaging*, 22(4):530–538, 2003.
- [7] H Becher, K Tiemann, T Schlosser, C Pohl, NC Nanda, MA Averkiou, J. Powers, and B. Luderitz. Improvement in endocardial border delineation using tissue harmonic imaging. *Echocardiography*, 15(5):511–517, 1998.
- [8] DN Rubin, N Yazbek, MJ Garcia, WJ Stewart, and JD Thomas. Qualitative and quantitative effects of harmonic echocardiographic imaging on endocardial edge definition and side-lobe artifacts. *J Am Soc Echocardiography*, 13(11):1012–1018, 2000.
- [9] R Senior, P Soman, RS Khattar, and A Lahiri. Improved endocardial visualization with second harmonic imaging compared with fundamental two-dimensional echocardiographic imaging. Am Heart J, 138(1 Pt 1), 1999.
- [10] F Chirillo, A Pedrocco, A De Leo, A Bruni, O Totis, P Meneghetti, and P Stritoni. Impact of harmonic imaging on transthoracic echocardiographic identification of infective endocarditis and its complications *Brit Med J*, 91(3):329–333, 2005.
- [11] C Caiati, N Zedda, C Montaldo, R Montisci, and S Iliceto. Contrast-enhanced transthoracic second harmonic echo doppler with adenosine A noninvasive, rapid and effective method for coronary flow reserve assessment J Am Coll Cardiol, 34(1):122–130, 1999.
- [12] S Hovda, H Rue, and B Olstad. New echocardiographic imaging method based on the bandwidth of the ultrasound Doppler signal with applications in blood/tissue segmentation in the left ventricle. *Computer Methods* and *Programs in Biomedicine*, 92(3):279–288, 2008.
- [13] RA Hager, DW Clark, KE Thiele, and JF Witt. Ultrasound clutter filter, June 22 2001. US Patent App. 09/887,648.
- [14] MA Lediju, MJ Pihl, SJ Hsu, JJ Dahl, CM Gallippi, and GE Trahey. A motion-based approach to abdominal clutter reduction. *IEEE Transactions on Ultrasonics, Ferroelectronics and Frequency Control, in press.*
- [15] M Hubert, PJ Rousseeuw, and K Vanden Branden. ROBPCA: a new approach to robust principal component analysis. *Technometrics*, 47(1):64–79, 2005.
- [16] CM Gallippi and GE Trahey. Adaptive clutter filtering via blind source separation for two-dimensional ultrasonic blood velocity measurement. *Ultrason Imaging*, 24(4):193–214, 2002.